PRODUCTION PROCESS

Algorithm-based design of mechanical joining processes

Mathias Jäckel[1] · Tobias Falk[1] · Welf-Guntram Drossel[1,2]

Abstract

In this paper, the development of algorithm-based process models for the mechanical joining process self-pierce riveting with semi-tubular rivet (SPR-ST) is described. Therefore, an extensive experimental and numerical database regarding the SPR-ST process and strength of steel and aluminum joints with tensile strengths of the sheets between 200 and 1000 MPa was generated for the building of the models. This process data could then be used for the training and evaluation of different prediction algorithms. Furthermore, the simulation data is applied to predict the entire contour (mesh) of non-simulated joints. This includes the visualization of output values such as strains, stresses and damage for each element and node of the mesh. That approach enables to obtain more information about the joint than just discrete values such as interlock or strength.

Keywords Self-pierce riveting · Numerical simulation · Machine learning

1 Introduction

Currently, the design of mechanical joining processes like self-pierce riveting with semi-tubular rivet (SPR-ST) for production involves time-consuming, experimental test series in which process parameters such as the rivet or die geometry are varied iteratively and based on experience until a suitable joint contour and strength is achieved. To simplify the use of mechanical joining technologies, these development cycles and thereby the effort for implementation into production must be reduced. Therefore, the goal of the research presented here is to enable an immediate prediction of the joint characteristics such as interlock formation and quasi-static strength or even the whole joint contour, based on the input parameters such as properties of the parts to be joined and process parameters.

This joining method can be divided in three steps as shown in Fig. 1. The first step is characterized by positioning the rivet and the sheets between the punch, blank holder and die (a). When the punch presses the rivet in the punch-sided sheet, the rivet pierces a slug out of the material, which

remains inside the cavity (b). The contour of the die forces the rivet to expand and an interlock is created (c). SPR-ST joints are evaluated by certain geometrical criteria (Fig. 1d). These criteria correlate with the strength properties of the joint and must fulfill specific values in order that the joint can be considered as proper [1].

In the past, the prediction of joining results was mainly focused on the numerical simulation of the SPR process. Numerous research works were carried out on the finite element method (FEM) process simulation for SPR-ST of mixed structures made of sheet metal materials. Contents of this work were e.g. the general improvement of functionality and prognosis accuracy of the process models [2], the numerical development of new rivet geometries [3], the determination of suitable process parameters [4] or the development of new process variants [5].

The progress due to the mentioned and other research work, the further development of simulation software systems and the constant advances in computer technology have contributed to the fact that the FEM simulation of SPR-ST of classical multi material joints made of sheet metal materials can be automated and carried out with high accuracy and with computing times of significantly less than one hour [6].

This opens up the possibility to perform a larger number of FEM calculations based on statistical design of experiments to be used as data to build regression models and analyze the SPR-ST process from a mathematical point of view [7], to use

✉ Mathias Jäckel
  Mathias.jaeckel@iwu.fraunhofer.de

1   Fraunhofer Institute for Machine Tools and Forming
    Technology IWU, Dresden, Germany

2   Professorship Adaptronics and Lightweight Design, TU
    Chemnitz, Chemnitz, Germany
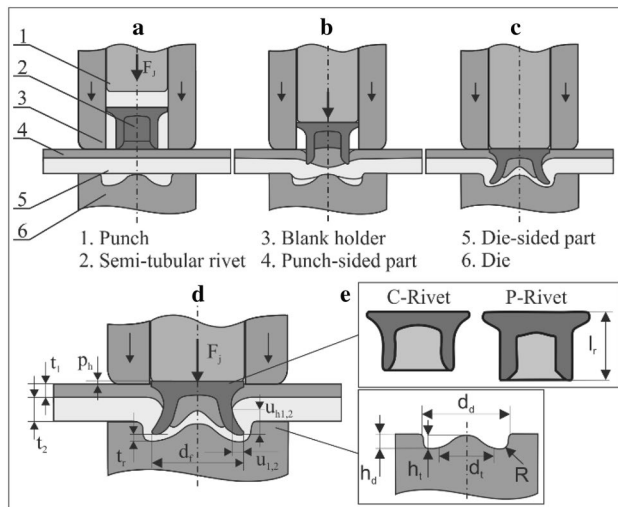
Fig. 1 Self-pierce riveting: **a–c** Process steps, **d** Characteristic values **e** Process parameters [1]

these models for atomization [8] or to reduce the number of necessary tools in production [9].

In terms of databased modelling in mechanical joining e.g. LAMBIASE in [10] used the data from 27 clinching process simulations to train an artificial neural network. In the investigations described, the prediction of the neural network could already be used for an optimization of process parameters. In [11], micrographs in combination with the joining force are used to train a convolutional neural network (CNN). The joining force was varied experimentally for two material-thickness combinations and three micrographs were created for each joining force. With the help of these image and process data, the neural network could be trained in order to subsequently predict a data-based forecast of the joining contour as a function of the joining force. For both material combinations, a very good prediction quality could be achieved in the tested area. In [12] neural network was trained and tested to classify which sheet thickness combinations for aluminum-steel combinations can be joined more or less successfully. Thereby also the influence of process parameters was taken into account.

The research described here aims to develop data-based predictive models for the SPR-ST process. Therefore, the necessary acquisition of the process data as well as the development of the prediction algorithms will be discussed in the following.

2 Experimental and numerical process data mining

Following, the SPR-ST process of steel and aluminum sheets is investigated. Thereby, the materials and thicknesses listed in Table 1 are considered.

For the experimental sampling, based on the materials of Table 1, 71 combinations were identified on the basis of a partial factorial experimental design according to the optimized latin hypercube sampling method [10]. Thereby the process parameters for each material combination was chosen by experience and the joint contour was obtained by means of micrograph preparations and measurement of the characteristic values (Fig. 1) [13]. In addition to the joint contour the quasi-static strength of the 71 material combinations was determined with respect to their load-bearing capacity in shear and top tension (Fig. 2) (three tests per material combination).

Due to the industrial relevance and comparability, the specimen forms are based on the simple shear and top tensile geometries according to [14]. In the test evaluation, the focus is on the maximum force F_{max} achieved in each load direction test.

For the generation of the numerical data, FEM (finite element method) simulation models for the joining process as well as the strength simulation (Fig. 3) were built and validated for each of the 71 experimentally joined material combinations for the SPR-ST process as well as the following quasi-static shear and top tensile tests. The boundary conditions for the simulation models for joining process can be found in [13]. The flow curves for the process simulation

Table 1 Considered specimen with mechanical properties

Material	$R_m/R_{p0,2}$ in MPa	Thickness in mm			
EN AW-6016 T4	≈ 240/129	0.8	1.15	1.5	2.0
EN AW-5182	≈ 287/144	1.15	1.25	1.5	2.0
CR210IF	363/241	0.8			
DX53D	≈ 287/144	1.0	1.25	1.5	1.75
HCT600XD	≈ 627/390	1.25	1.5	1.75	2.0
HCT780XD	1035/622	1.25			
HCT980XG	1022/865	1.0			
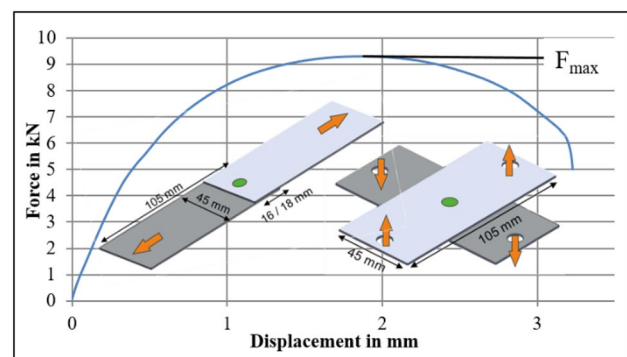
Fig. 2 Example of force–displacement curve and geometries used for the quasi-static strength tests [11]

were conducted via stack compression test for each considered material [15].

For the numerical simulations of the SPR-ST process with the following strength calculation, the software Simufact Forming is used due to the short computation times as well as good automation capability. When building the models, the focus is on computational efficiency, low manual effort during the build-up and the best possible accuracy. Therefore, objects for the following top and shear tensile

Fig. 3 Structure of the models for the strength simulation of the SPR-ST process

simulation are already taken into account when setting up the 2D joining simulation (Fig. 3).

This means that the joining result of the 2D joining simulation can be integrated into the model structure of the strength test with relatively little effort, and the load calculation can be performed immediately. Due to the extensive number of materials considered and the simplicity of calibration, specimen failure was modeled in the simulation using the Cockroft & Latham macro-mechanical damage criterion [16] by calibrating the damage value with the experiments. Overall, the simulation models for joining process and strength simulation were built and calculated for all 71 material combinations investigated in the experimental studies.

In the here described investigations the main objective of the numerical data acquisition is to generate as comprehensive and representative a set of data describing the joint formation and the quasi-static strength behavior of SPR joints of the sheet materials under consideration. In order to limit the effort in numerical model building and calculation times, sacrifices in terms of accuracy have to be tolerated.

Table 2 shows the average absolute and magnitude deviations (Δ) between the experiments and simulations for the best (lowest deviation to the experiments) 50 of 71 originally build up simulation models. The geometric parameters of the joint contour (Fig. 1) and the maximum forces in the top tensile test F_{maxTT} and in the shear tensile test F_{maxST} (Fig. 2) are evaluated.

On average, the deviation of the joint contour is approx. 18.8% and for the quasi-static joint strength approx. 18.6%. Due to the acceptable agreement between experiment and simulation, these 50 simulation models were used for the numerical variation calculations. Therefore material properties conditions like material flow curve, sheet thickness, die and rivet geometry were varied [13]. In total, based on a statistical experimental design, 19 variations per simulation model were built and calculated for the strength calculations, resulting in a total of 1.000 simulation models for the SPR-ST process with the following strength calculation. However, after a technological review of the simulation results, a large number of calculation results could not be taken into account for the development of the data-based models due to e.g. missing interlock formation, material penetration or rivet compression. Therefore, numerical joining results of 2.376 different material combinations from previous investigations
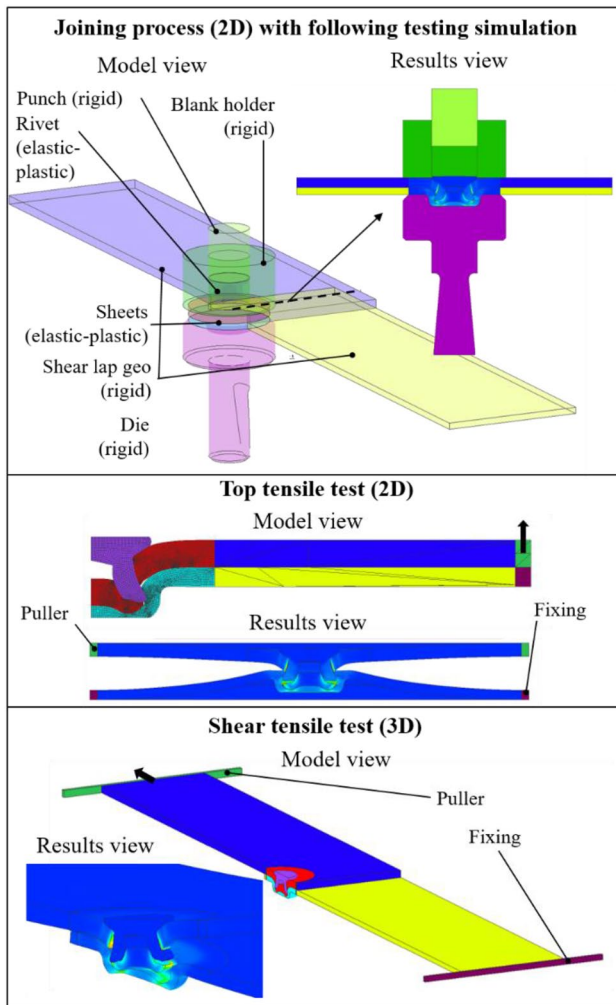
Table 2 Deviation between experiments and numerical results for joining process and strength simulation for 50 SPR-ST joints

	Joint contour				Joint strength	
	$u_{1,2}$	$u_{h1,2}$	t_r	d_f	F_{maxTT}	$F_{max\ ST}$
Δ in %	− 8.9	− 13.5	3.2	0.3	1.3	21.4
$|\Delta|$ in %	25.5	24.0	21.9	2.2	13.1	23.9
$\overline{X}|\Delta|$ in %	18.8				18.6	

[13] for the geometric criteria of the joint contour and 771 material combinations with strength testing are available for the analysis of the prediction models.

3 Joint characteristics and strength prediction

Different algorithms (Table 3) are tested for the prognosis of the geometrical joint characteristics (2.376 datasets) and the strength prognosis (771 datasets).

Therefore, the data set is randomly split in a training set (80% of all data) to train the models and a test set (remaining 20%). With these test data, a comparison of original (y_i) and predicted $(\hat{y}_i)$ values can be executed, and, with the coefficient of determination R^2 (1), all models can be compared and rated ($\bar{y}$ mean value). Thereby the range of R^2 is $0 \leq R^2 \leq 1$ (1 is best possible evaluation). [13]

$$R^2 = 1 - \frac{\sum \left(y_i - \hat{y}_i\right)^2}{\sum \left(y_i - \bar{y}\right)^2} \tag{1}$$

The closer original and predicted values are, the higher of R^2 and the better the quality of prediction model.

For the training of the algorithms for the prognosis of the geometrical characteristic values, the material properties, process parameters serve as input data (Table 4). In the case of strength prediction, the geometric characteristic values are also considered as input variables.

When analyzing which algorithms are best suited for the different data sets and structures, R^2 is determined separately for each output parameter and the mean value for the joint contour and strength is calculated (Table 5). Thereby the implementation of the algorithms is based on the open source python library scikit-learn [17].

For both the joint contour and the strength, the Gradient Boosted Decision Tree (GBDT) algorithm performs the best prognosis quality with R^2 of approx. 0.9. Thereby different hyper parameters like learning rate, number of boosting

Table 3 Considered algorithms and the respective number of hyper parameter variations [13]

Algorithm	Hyper parameter variations
Linear regression (LR)	1
Huber regression (HR)	36
Support vector regression (SVR)	40
k-nearest-neighbor (kNN)	40
Gradient boosted decision tree (GBDT)	9
Multilayer perceptron—artificial neural network (MLP)	27

Table 4 Input and output data for the training of the algorithms

Category	Characteristic value
Material properties	Ultimate tensile strength
	Sheet thickness
	Type of material (steel, aluminum)
Process parameters	Die contour (d_d, h_d, d_t, h_t, R)
	Rivet type and length (C/P-rivet, l_n)
	Rivet head position (p_h)
Geometrical joint characteristics	Interlock $u_{1,2}$
	Interlock height $u_{h1,2}$
	Min. thickness die-sided part t_r
	Rivet foot diameter d_f
Joint strength	Max. top tensile force F_{maxTT}
	Max. shear tensile force F_{maxST}

stages and maximum depth and number of nodes in the tree were implemented and tested [17]. With boosting methods, such as GBDT, base estimators are sequentially built and one tries to reduce the bias of the combined estimator. The motivation is to combine several weak models to produce a powerful ensemble. GBDT is a generalization of boosting to arbitrary differentiable loss functions [18]. In Fig. 4 the prognosis quality of Linear Regression, Gradients Boosting Decision Tree and Multilayer Perceptron are compared, trained with varying amount of data (experimental and numerical strength results).

It can be noted that the simpler linear regression model achieves better prediction qualities with the smaller number of data sets from the experiments. However, the forecast quality with $R^2 = 0.61$ is insufficient. With the availability of a larger number of data sets, the more complex regression
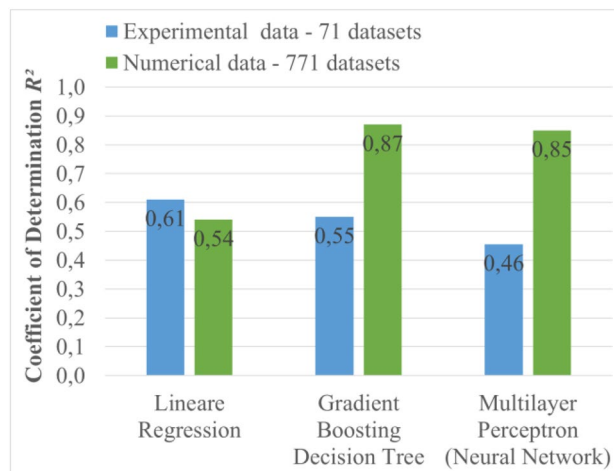
Fig. 4 Comparison of the coefficient of prognosis R^2 for different regression algorithms trained with varying amount of data

Table 5 Comparison of the coefficient of determination R^2 of the considered algorithms for joint characteristics and joint strength

Algorithm	Joint contour (2.376 data sets)					Joint strength (445 data sets)		
	$u_{1,2}$	$u_{h1,2}$	t_r	d_f	$\overline{X}$	$F_{max\ TT}$	$F_{max\ ST}$	$\overline{X}$
LR	0.72	0.81	0.57	0.80	0.73	0.37	0.65	0.51
HR	0.73	0.82	0.57	0.81	0.73	0.49	0.68	0.59
SVR	0.62	0.65	0.53	0.48	0.57	0.30	0.52	0.41
k-NN	0.36	0.41	0.40	0.37	0.39	0.32	0.56	0.44
GBDT	0.91	0.90	0.86	0.94	0.90	0.85	0.88	0.87
MLP	0.55	0.80	0.53	0.62	0.63	0.66	0.84	0.75

models such as GBDT and MLP show a significant increase in prediction accuracy.

4 Prediction and visualization of entire joint contours and output parameters

In the previous section, the numerically generated data sets have been used to predict only discrete values such as geometrical characteristics or strength properties. The next step goes beyond this and allows the prediction of the complete joint contour. In addition to the pure geometric predictions, it is also possible to predict and visualize damage, stresses or strains, just as commercial simulation software provides. The advantage of the prognosis shown here is the extremely short calculation time (< 1 s) and the intuitive use without the need of a proven expertise. Therefore, the database with the 2.376 simulations of the SPR-ST process [13] is used as foundation.

Since all simulation meshes have a different structure and also the number of nodes and elements are inconsistent, a standardization of the individual joining partners as well as the rivet must be implemented first for comparability to achieve a uniform design of the resulting meshes. Using the example of the rivet, Fig. 5 shows how this standardization is carried out: The outer contour of the initial mesh is divided

into equidistant distances and into upper and lower contours. The connections between two nodes belonging to each other are again divided into equal distances and thus the inner, standardized nodes are created.

As already mentioned, it should also be possible to predict output variables such as maximum principal stress. Therefore, a mapping of the node information from original to standardized mesh structure is necessary (Fig. 6). Since each new node (gray) is located in a triangle of original nodes (black), the value of the output parameter at this point can be determined by ratios of the sides, thus a classical linear interpolation. Since the individual nodes are close together and the values of the output parameters of neighbored nodes do not change abruptly, possible errors during the mapping are marginal and negligible.

Figure 7 compares the calculation results between the original and mapped mesh using the example of the max. principal stress. A very good correlation can be achieved.

The standardization of the simulation mesh includes 4.928 nodes. Since a total of 2.376 simulations are integrated, data reduction is indispensable for fast prediction and visualization. Therefore, linear principal component analysis [19, 20] is used. With regard to a balanced ratio of computation time and accuracy, 30 principal components are determined for further consideration. Considering that the complexity with this small number of principal components

Fig. 5 Original simulation mesh of a rivet (left); standardized mesh of the same rivet (right)
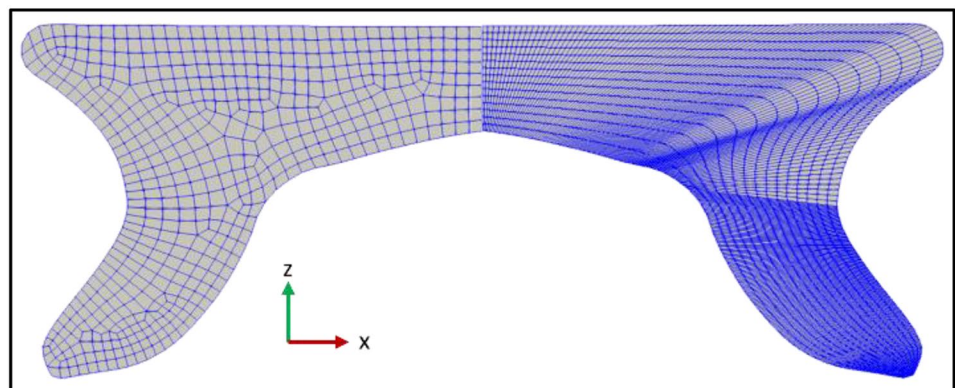
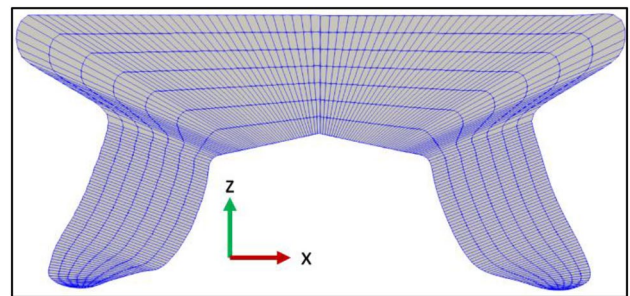**Fig. 6** Mapping output values from original mesh to standardized nodes
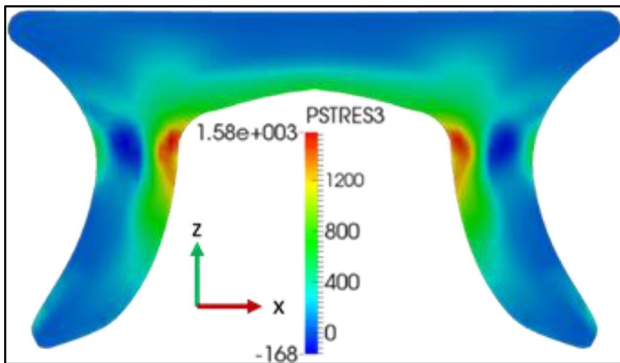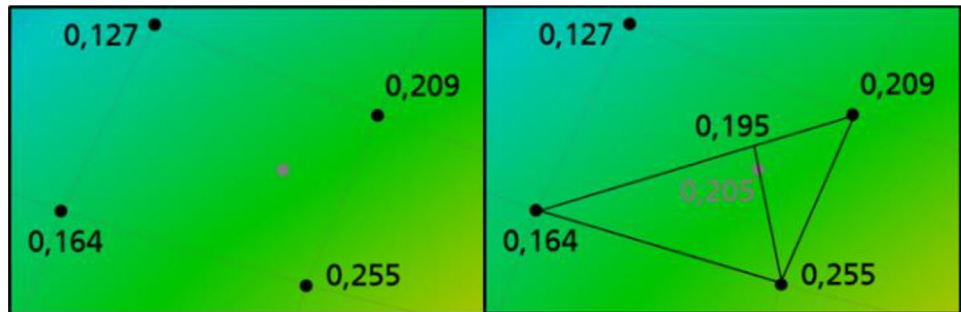
Fig. 7 Visualization of maximum principal stress: original mesh (left); mapping to standardized mesh (right)

Fig. 8 Standardized mesh (left); with 30 principal components calculated mesh (right)

compared to the total number of simulations is close to 1.3%, the results obtained with this approach are sufficiently good (Fig. 8).

With this reduced number and complexity, an individual prediction model is created for each principal component. Different polynomial approximation approaches (Table 6) [21] are examined with respect to a best possible prediction and compared by means of the explained coefficient of determination (1). The approximation coefficients determined in this way are saved and passed on for the prediction. For the visualization of the results in their original form, the data-reduced values have to be transformed back. The coefficient of determination for the prediction of the node points respectively the connection contour lies with 89% in a high confidence range. For the calculation of the output quantities to be visualized, it lies in the range between 60 and 80% depending on the considered parameter.

Remarkably, despite the significant data reduction, SPR-ST joints are clearly recognizable in the nodes and geometries calculated in this way (Fig. 9). Furthermore, changes in the input parameters are also predicted accordingly and reflected in the results.

Table 7 shows the changes in the input parameters, and their effects on the predicted results are represented in Fig. 9. Comparing the two designs, the reduced blank sheet thicknesses t_1 and t_2 are evident, as are the reductions in die

Table 6 Integrated polynomial approximation approaches

Approximation approach	Mathematical expression
Linear basis	$r_0 + \sum_{i=1}^{n} r_i \bullet x_i$
Linear basis with mixed terms	$r_0 + \sum_{i=1}^{n} r_i \bullet x_i + \sum_{i,j=1,j>i}^{n} r_{ij} \bullet x_i \bullet x_j$
Quadratic basis	$r_0 + \sum_{i=1}^{n} r_i \bullet x_i^2$
Linear and quadratic basis	$r_0 + \sum_{i=1}^{n} r_i \bullet x_i + \sum_{j=1}^{n} r_j \bullet x_j^2$
Linear and quadratic basis with mixed terms	$r_0 + \sum_{i=1}^{n} r_i \bullet x_i + \sum_{i,j=1,i\geq j}^{n} r_{ij} \bullet x_i \bullet x_j$

diameter d_d and depth h_d, and thorn diameter d_t and height h_t. In addition, it can be seen that the general rivet shape R (value 1 corresponding to C-rivet, value 2 corresponding to P-rivet), rivet length l_r and rivet head position p_h are taken into account and transferred by the prediction.

Analogous to the presented prediction results of horizontal x and vertical z coordinates of each node, the output information of damage, stresses and strains are also calculated in this way for each node.

In order to effectively use, the described method for the prediction of SPR-ST joint formation, standardization, data reduction and prediction modeling have been incorporated into a software demonstrator (Fig. 10). This allows the values of the sheet properties, die and rivet geometry to be set in a simple way by sliders, and the predicted joint formation including the chosen results (e.g. damage) is visualized in real time.

Fig. 9 Predicted SPR-ST geometries
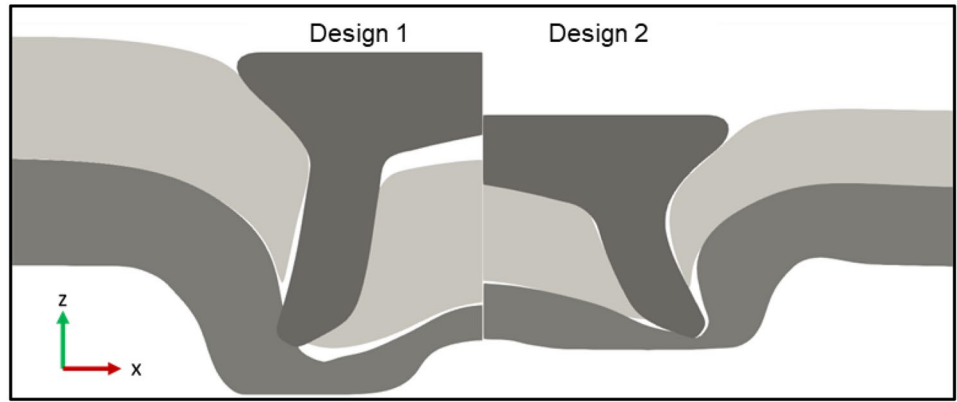
Table 7 Values of input parameter

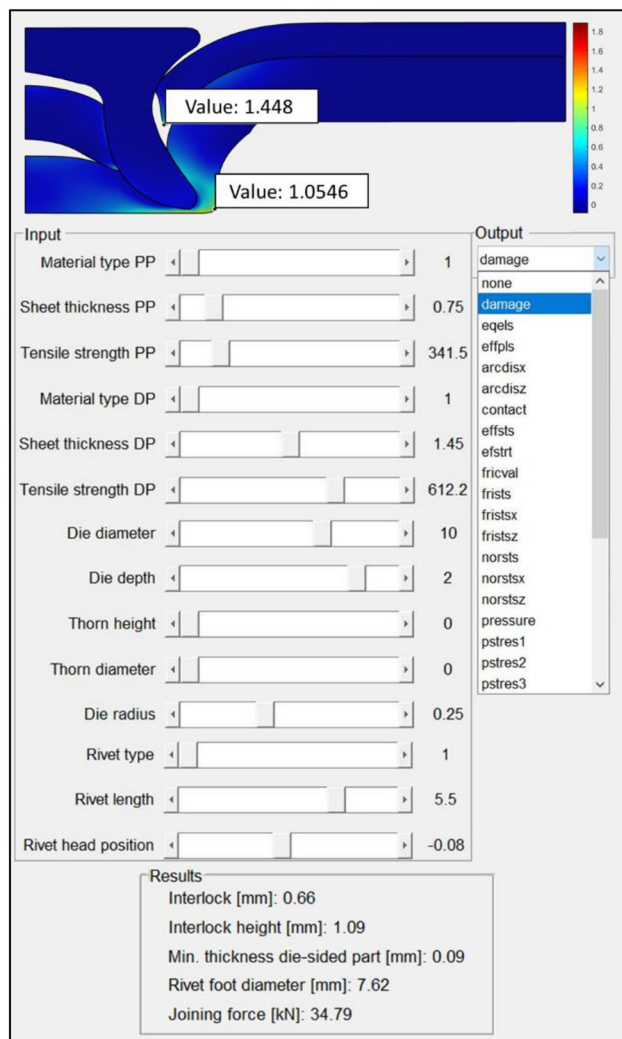| Design	t_1	t_2	d_d	h_d	d_t	h_t	R	l_r	p_h
1	1.85	1.6	11	2	4	1	2	5	− 0.22
2	1.2	1.2	9	1.4	0	0	1	4	0

Based on the displayed SPR-ST joint, the characteristic parameters (Fig. 1d) such as interlock and min. material thickness of the die-sided sheet are automatically calculated and shown. In addition, it is possible to display the predicted values of the currently selected output parameter (here: damage—Cockroft & Latham [16]) for different nodes by mouse click. When selecting a different output parameter (e.g. maximum deformation or maximum principal stress), these nodes remain selected and the values of the newly selected parameter are displayed.

5 Summary and outlook

The research results described here demonstrate the potential of algorithm-based prediction of joining results. The availability of comprehensive and high-quality material and process data is essential for the development of reliable models. In the case of SPR-ST, numerical simulation can be used for the necessary data acquisition due to its good numerical accuracy, relatively short computing times and good automation capabilities. In this survey, the GBDT algorithm provides the best prediction results for geometric parameters and joint strength with the generated process data. The developed method for the prediction of joining point contours including output values has high potential in sampling support. The presented software demonstrator allows simple and intuitive parameter input and generates numerically appearing joining points in real time.

With regard to the industrial implementation of the approaches developed, it was shown that generally available material data such as tensile strength and sheet thicknesses, as well as the known process parameters, enable good predictions to be made for both the joint contour and joint strength. The next step is to test the developed models in practice and to develop an application-related graphical interface for the use of the prediction models. Based on these field tests, the ideal application areas can be identified and any deviations related to different material classes can be determined.

Fig. 10 Software demonstrator (*PP* punch-sided part, *DP* die-sided part)

References

1. DVS, EFB 3410 (2018) Merkblatt Stanznieten-Überblick. DVS-Verlag, Düsseldorf
2. Hahn O, Dölle N (2001) Numerische Simulation des Füge-prozesses beim Stanznieten mit Halbhohlniet von duktilen Blech-werkstoffen, Dissertation, Shaker Verlag, Aachen
3. Uhe B, Kuball CM, Merklein M et al (2020) Improvement of a rivet geometry for the self-piercing riveting of high-strength steel and multi-material joints. Prod Eng Res Devel 14:417–423
4. Mori K, Abe Y, Kato T (2014) Self-pierce riveting of multiple steel and aluminium alloy sheets. J Mater Process Technol 214:2002–2008
5. Kraus C, Falk T, Mauermann R et al (2020) Development of a new self-flaring rivet geometry using finite element method and design of experiments. Procedia Manuf 47:383–388
6. Raabe M, Mente M (2016) HiVoFlex—Effective integration of virtual process design into a high volume high flexible automotive production concept. Simulation 2016, Bad Nauheim
7. Tassler T, Israel M, Goede M et al (2017) Verbesserung der Vor-hersagegenauigkeit von Metamodellen. Forsch Ingenieurwes 81(4):373–382
8. Jäckel M, Falk T, Landgrebe D (2016) Concept for further development of self-pierce riveting by using cyber physical systems. Procedia CIRP 44:293–297
9. Falk T, Jäckel M (2019) Process optimization for flexible self-pierce riveting of multi-material structures. AIP Conf eedings 2113(1):050011
10. Lambiase F, Di Ilio A (2014) Optimization of the clinching tools by means of integrated fe modelling and artificial intelligence techniques. Procedia CIRP 12:163–168
11. Oh S, Kim HK, Jeong T-E, Kam D-H, Ki H (2020) Deep-learning-based predictive architectures for self-piercing riveting process. IEEE Access 8:116254–116267
12. Karathanasopoulos N, Pandya KS, Mohr D (2021) Self-piercing riveting process: Prediction of joint characteristics through finite element and neural network modeling. J Adv Join Process 3:100040
13. Jäckel M, Falk T, Georgi J, Drossel WG (2020) Gathering of process data through numerical simulation for the application of machine learning prognosis algorithms. Proc Manuf 47:608–614
14. DVS, EFB 3480–1 (2021) Merkblatt Prüfung von Verbindung-seigenschaften Prüfung der Eigenschaften mechanisch und kombiniert mittels Kleben gefertigter Verbindungen. DVS-Verlag, Düsseldorf
15. Jäckel M, Coppieters S, Vandermeiren N et al (2020) Process-oriented flow curve determination at mechanical joining. Proc Manuf 47:368–374
16. Cockroft MG, Latham DJ (1968) Ductility and workability of metals. J Inst Met 96:33–39
17. https://scikit-learn.org/stable/supervised_learning.html#supervised-learning, Accessed 7 Oct 2021
18. Friedman JH (2002) Stochastic gradient boosting. Comput Stat Data Anal 38:367–378

19. Pearson K (1901) On lines and planes of closest fit to systems of points in space. Philosophical Magazin 2:559–572
20. Hotelling H (1933) Analysis of a complex of statistical variables into principal components. J Educ Psychol 24(6):417–441
21. Clarkson JA, Erdös P (1943) Approximation by polynomials. Duke Math J 10(1):5–11

Publisher's Note Springer Nature remains neutral with regard to jurisdictional claims in published maps and institutional affiliations.